Pseudo volume-plasmon in arrays of doped and un-doped semiconductors

Thierry Taliercio*, Vilianne N'Tsame Guilengui, and Eric Tournié

Institut d'Electronique du Sud, CNRS-INSIS-UMR 5214, Université Montpellier 2,
34095 MONTPELLIER cedex 05 (France)
*corresponding author, E-mail: thierry.taliercio@univ-montp2.fr

Abstract

We present a theoretical work which shows that for a metamaterial consisting of a periodic array of doped and undoped semiconductors it is possible to define a frequency ω_t corresponding to a pseudo volume-plasmon. ω_t depends on the thicknesses and on the dielectric constants of the components of the metamaterial and on the plasma frequency of the doped semiconductor. As its homologue in noble metal, the pseudo volume-plasmon is the collective oscillation of charges present in the metallic part of the metamaterial leading to a pure longitudinal electric wave. We show that ω_t is the degeneracy frequency between the anti-symmetric mode in transverse magnetic field (TM) and the mode in transverse electric field (TE). We demonstrate that this degeneracy is due to the periodicity of the structure which transforms the imaginary solution of a metal-dielectric interface into a real solution in the case of the periodic metamaterial.

1. Introduction

Recent developments of plasmonics have opened new prospects to control light-matter interactions [1,2]. Surface plasmon polaritons (SPP) result from the coupling between an electromagnetic wave and the collective oscillation of the electrons supported by the metal/dielectric interface. They exhibit unique physical properties due to enhanced nanolocalized optical fields. In the past decade, several breakthroughs have been made to improve the control of the wave propagation via wave-guides [3], plasmonic crystals [4,5] or the so-called extraordinary optical transmission (EOT) [6]. More recently, new applications have been proposed which are based on the exaltation of the electromagnetic field near metallic surfaces. They allow to enhance natural optical properties of materials [7] or to generate nonlinear effects by breaking symmetries [8,9] and induce a control of the optical processes at the femto-second scale [10,11].

The existence of the SPP, and their unique optical properties, is possible because of the presence of the volume plasmon with its characteristic frequency, ω_p. Volume plasmon is a quantum of the oscillating plasma and a pure longitudinal electric wave propagating into the metal. This particular wave can be excited uniquely by electrons, because of its longitudinal nature, by coupling between the electric charge of the electron and the fluctuations of the electrostatic field of the plasma wave. It is necessary to use energy electron loss spectroscopy (EELS) to characterize volume plasmon [12-14]. An indirect signature can be obtained in optical reflectance spectra because the dielectric function equals 0 for $\omega = \omega_p$. But generally this method is limited to doped semiconductors [15] because ω_p is in the deep UV range and is masked by the inter-band absorption for noble metal. Controlling the plasma frequency is fundamental for engineering the optical properties of new photonic devices. It is possible to adjust the volume plasmon frequency in the microwave range notably by using thin-wire structures [16-18]. However, realizing three-dimensional (3D) structure for IR applications is difficult because of technological limitations. It is, however, possible to investigate simpler one or two dimensional structures to control the plasma frequency ω_p.

In the case of one dimensional structures such as grids of parallel metallic wires, theoretical works have been done to explain in detail their optical properties [19,20]. They consider structures with a period d larger than l, the aperture of the grating, and much larger than the plasma wavelength λ_p. In other words, $\lambda_p << l < d$. They have shown that their main optical property, the EOT, is due to the coupling of the incident plane wave with cavity resonances located inside the slits, leading to localized SPP, or to the excitation of coupled surface electromagnetic modes on both surfaces of the grid, resulting in coupled SPP (see ref. 21 for more detail).

Theoretical studies dealing with comparable λ_p, l, and d, have been performed on infinite or truncated super-lattices of metal/dielectric or semiconductor/semiconductor [22-25]. They showed in the case of truncated super-lattices that bulk and surface plasmon should exist because of periodicity. The term bulk and surface plasmon are used to describe the coupling through the structure of surface plasmon pinned at each interface and surface plasmon pinned at the truncated surface, respectively. Such works, however, did not investigate the impact of the carrier

density modification given by the fraction of space occupied by the metal.

Recently, this theoretical approach has been simplified and an analytic model has been proposed to treat periodic arrays of doped and un-doped semiconductors in the long wavelength limit to exploit the polaritonic behaviour of the SPP [26]. The main difference between Ref. 26 and previous works on periodic slit arrays is that Ref. 26 considers the case where d << λ_p. This implies fundamental differences: it is no more possible to consider the metal as a perfect conductor and the zero order transmission or reflection is at higher frequency than the plasma frequency. So the optical properties of doped and un-doped semiconductor arrays are essentially governed by SPP located inside the un-doped semiconductor part. One of the main results of this analytic model was to demonstrate the existence of a huge photonic band gap which opens the possibility to realize optical filtering in the IR and THz ranges. Similar structures based on metal and dielectric waveguides have been first studied in 1969 [27]. Three branches appeared in the dispersion relation, two of them corresponding to the symmetric modes and one to the anti-symmetric mode. Several other works have completed the theoretical study of SPP wave-guides [28-29]. However, the quasi-bi-dimensional shape of wave-guides makes them difficult to manipulate in free space optic. Periodic arrays in contrast allow avoiding this problem and give access to new optical properties like negative refractive index [30-34] or high index of refraction [35] and particularly in the case of using highly doped semiconductors. Indeed, it is possible to adjust the plasma frequency, ω_p, that give an additional degree of freedom to control the permittivity, ε, from the IR to the THz range [36,37].

In this work, we propose a theoretical work on pseudo volume-plasmons which can be observed in periodic arrays of doped and un-doped semiconductor. We first describe the theoretical framework and highlight the analogy between a SPP and an ionic crystal (Sec. II). We then generalize this approach to periodic structures before defining the concept of pseudo volume-plasmon and studying its properties (Sec. III). Finally, we propose a scheme of the pseudo volume-plasmon (Sec. IV) and discuss the physical meaning of the pseudo volume-plasmon frequency in light of the ionic-crystal analogy (Sec. V).

2. Surface Plasmon Polaritons modeled as an ionic-crystal

2.1. SPP at the metal/dielectric interface

We consider the interface between two semi-infinite materials as depicted in Fig. 1. For simplicity, we normalize all frequencies to the plasma frequency ω_p, the wave numbers to $k_p = \omega_p / c$, the lengths (including spatial variables) to k_p^{-1}, and time to ω_p^{-1}.

The index of the structure is defined as:

$$n^2(z,\omega) = \begin{cases} \varepsilon_b \ for \ z > 0 \\ \varepsilon' = \varepsilon_a \left[1 - \frac{1}{\omega(\omega + i\gamma)}\right] \ for \ z < 0 \end{cases}, \quad (1)$$

where a Drude dielectric function is used to model the behaviour of the doped semiconductor.

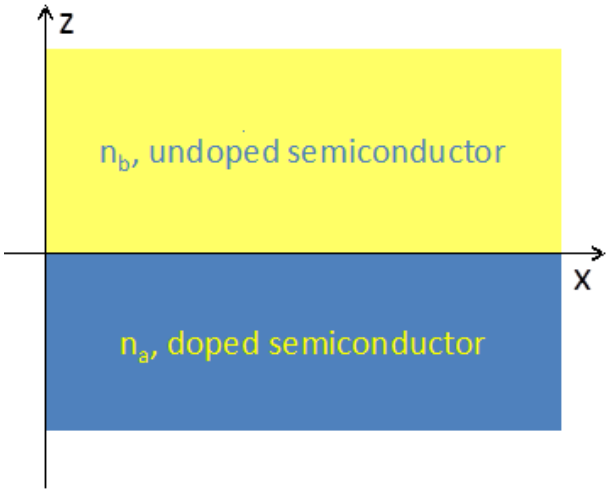

Figure 1: Scheme of the structure corresponding to an interface (x axis) between two materials which are assumed to be semi-infinite in the z direction and infinite in the y direction. The indexes of the doped and un-doped semiconductors are respectively $n_a = \sqrt{\varepsilon'}$ and $n_b = \sqrt{\varepsilon_b}$. The SPP propagates along the x direction.

We consider that the TM field exciting the surface wave that propagates along the interface takes the form:

$$\vec{E}(x,z,t) = \begin{pmatrix} E(z) \\ 0 \\ F(z) \end{pmatrix} e^{i(\omega t - qx)}. \quad (2)$$

We study the dependence with the z variable. Computing $\nabla \times \nabla \times \vec{E}(x,z,t)$ in the Maxwell equation $\nabla \times \nabla \times \vec{E} + (n^2/c^2)\partial_t^2 E = 0$, and eliminating $\partial_z F(z)$, we obtain the usual Helmotz equation for E(z), and an explicit expression for F(z):

$$\frac{\partial^2 E}{\partial z^2} + [n^2(z,\omega)\omega^2 - q^2]E = 0, \quad (3)$$

$$[n^2(z,\omega)\omega^2 - q^2]F = -iq\frac{\partial E}{\partial z}. \quad (4)$$

Considering the boundary conditions at the interface, that is the continuities of the field components $E_{//}$, $B_{\perp}$, the discontinuities of the field components $E_{\perp}$, $B_{//}$ and the Gauss theorem for z < 0, $(\nabla\left(\varepsilon'\overrightarrow{E_a}(x,z,t)\right) = 0)$ and for z > 0, $(\nabla(\varepsilon_b\overrightarrow{E_b}(x,z,t)) = 0)$ allow collecting 6 equations. Manipulating these equations allows obtaining the well-known equation:

$$\frac{\varepsilon_b}{k_b} - \frac{\varepsilon'}{k_a} = 0, \quad (5)$$

where k_a and k_b are respectively the wavenumbers for z < 0 and z > 0 and are given by:

$$k_a^2 = \varepsilon_a(\omega^2 - 1) - q^2, \quad (6)$$

$$k_b^2 = \varepsilon_b \omega^2 - q^2. \quad (7)$$

For more detail the reader should refer to [1]. Injecting Eq. (6) and (7) in (5) gives:

$$q^2 = \frac{\varepsilon_a \varepsilon_b}{\varepsilon_a + \varepsilon_b} \frac{\omega^2 - 1}{\omega^2 - \omega_s^2} \omega^2, \quad (8)$$

where $\omega_s^2 = \frac{\varepsilon_a}{\varepsilon_b + \varepsilon_a}$. (9)

Eq. (8) and (9) are respectively the dispersion relation ω(q) and the expression of the SPP frequency at the metal/dielectric interface.

2.2. Analogy between SPP and ionic crystal

Let us compare the dispersion relation ω(q) in Eq. (8) to the one found in ionic crystals. Ashcroft & Mermin [38] define it in chapter 27 formulae (27.57) and (27.67):

$$\varepsilon(\omega) = \varepsilon_\infty + \frac{\varepsilon_\infty - \varepsilon_0}{(\omega^2/\omega_T^2) - 1}, \quad (10)$$

$$\omega_L^2 = \frac{\varepsilon_0}{\varepsilon_\infty} \omega_T^2, \quad (11)$$

where ε_0 and ε_∞ are the dielectric constants at low and high frequencies and the subscripts L and T are meant for *Longitudinal* and *Transverse*. Eq. (11) is the so-called *Lyddane-Sachs-Teller relation*. Combining these two relations gives

$$\varepsilon(\omega) = \varepsilon_\infty \frac{\omega^2 - \omega_L^2}{\omega^2 - \omega_T^2}. \quad (12)$$

Taking into account $\omega^2 = c^2 q^2 / \varepsilon(\omega)$, we obtain:

$$q^2 = \epsilon_0 \mu_0 \omega^2 \varepsilon_\infty \frac{\omega^2 - \omega_L^2}{\omega^2 - \omega_T^2}, \quad (13)$$

where ϵ_0 and μ_0 are the permittivity and permeability of the vacuum.

Now Eq. (13) is exactly the expression of the dispersion relation given above in Eq. (8) provided that:

$$\varepsilon_\infty = \frac{\varepsilon_a \varepsilon_b}{\varepsilon_a + \varepsilon_b}, \quad (14)$$

$$\omega_L = \omega_p, \quad (15)$$

$$\omega_T = \omega_s. \quad (16)$$

The dielectric constant at high frequencies of the composite material considered in the ionic-crystal model is an average between these of the metal and of the dielectric. If both dielectric constants are equal we obtain the well-known value of the SPP frequency in the case of an interface between a noble metal and the air, $\omega_p/\sqrt{2}$. The longitudinal frequency, associated to the zero of the dielectric function (Eq. (13)), corresponds to the plasma frequency which is of course a pure longitudinal electric wave. The transverse frequency, associated to a pole of the dielectric function (Eq. (13)), corresponds to the SPP frequency. In fact, this is the oscillator frequency (or the two level system) necessary to develop the crystal-ionic model. Thus, we can view the SPP as an oscillator pined at the interface between the metal and the dielectric. Finally, considering the *Layddane-Sachs-Teller* relation, we can define the dielectric constant at low frequencies

$$\varepsilon_0 = \varepsilon_b, \quad (17)$$

As expected for an ionic crystal, ε_∞ is smaller than ε_0. In addition, ε_0 is simply due to the contribution of the dielectric material. This stems from the fact that the electromagnetic wave does not penetrate the metallic part which can be considered as a perfect conductor at low frequencies.

2.3. The SPP dispersion relation ω(q)

Let us consider the dispersion relation eq. (8) which is valid for both real and imaginary solutions of the wave-vector **q**. As an example we show in Figure 2 the solutions obtained when both ε_a and ε_b dielectric constants are taken equal to 11.7 (which is the value of InAs). The real and imaginary solutions are the black and the red-dashed lines, respectively. The SPP frequency is noted ω_s. In the low frequency range (lower than ω_s), we can recognize the dispersion relation law of the SPP which corresponds to the bound mode at the interface. Frequencies higher than 1 correspond to the radiative regime into the metal. At these frequencies, the metal is transparent. When the normalized frequency lies between ω_s and 1, we obtain a photonic band gap, a range of frequencies where the wavenumber is purely imaginary. No mode is sustained at the interface. The inset in figure 2 shows the x and z components of the electric field through the interface. Note that the electric field of the unique SPP mode is pined at the interface (E_x component). This is the only possible mode at the interface.

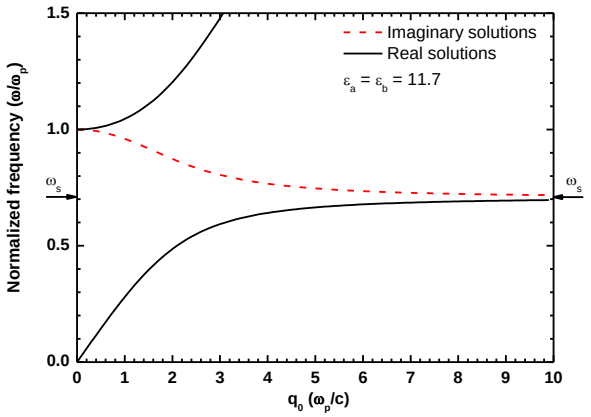

Figure 2: Dispersion relation of SPP at the interface between a doped semiconductor and an un-doped semiconductor. The dielectric constants are equal to 11.7. The dark lines and the red dashed line correspond respectively to the real and the imaginary solutions of eq. (8). The SPP frequency is noted ω_s. Inset shows the z and x components of the electric field along the z axe of the SPP.

We will see in the following that this mode can be compared to the symmetric mode of wave-guide [27] or of periodic structures [26,32] whereas the imaginary solution should be

compare to the anti-symmetric one. Indeed, for these cases several modes can be sustained. We develop this point in the next section.

3. The periodic array of doped and un-doped semiconductors

We now extend the point of view of the ionic-crystal model to periodic arrays. Let us recall the main results of ref. 26 obtained in the long wavelength limit approximation. Indeed, the main difference between this approach and previous ones [19-21] is the fact that λ_p is larger than the grating period (a + b). This implies, first, the selection of vertical SPP into the un-doped semiconductor and, second, the possibility to obtain SPP modes nears the plasma frequency.

Consider the metamaterial composed of a periodic array of doped and un-doped semiconductors (Fig. 3-a and c). When light is under normal incidence, this metamaterial may be considered as ionic-crystal in TM field and as a metal in TE field (Fig. 3-b and d). To reach these results it is necessary to consider the dielectric function and the thickness of the doped (ε' and a) and un-doped (ε_b and b) semiconductors as follows:

$$n^2(z,\omega) = \begin{cases} \varepsilon_b \ \ for \ z \in [-b, 0] \\ \varepsilon' = \varepsilon_a \left[1 - \frac{1}{\omega(\omega+i\gamma)}\right] \ \ for \ z \in [0, a] \end{cases}. \quad (18)$$

The doped semiconductor follows a Drude model whereas in the case of the un-doped one we consider its dielectric constant. Afterwards, it is necessary to solve the Maxwell equations in each region and consider the boundary conditions in both interfaces. Several mathematical manipulations are necessary to obtain the dispersion relation in both cases

$$q^2 = \varepsilon_{eff}\omega^2 , \quad (19)$$

where q is the wavenumber and ε_{eff} the effective dielectric function.

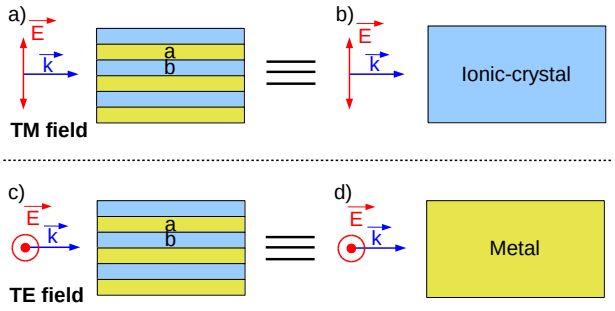

Figure 3: Schemes of the simplification obtained by the model of ref. 26. The periodic arrays of doped and un-doped semiconductors can be view as ionic-crystal under TM filed radiation, a) and b), or as a metal under TE field radiation, c) and d). Materials a and b stand for metal and dielectric, respectively.

Note that the term effective dielectric function, ε_{eff}, is very restrictive because it is valid for normal incidence or close to the normal incidence. ε_{eff} is well defined essentially along the x direction and is strongly polarization depend. Indeed, in TM field, ε_{eff} follows the ionic-crystal model with characteristic dielectric constant ε_{TM} and frequency ω_r. ε_{TM} and ω_r correspond respectively to the average dielectric constant and to the frequency associated to the oscillators pined at the interface:

$$\varepsilon_{eff} = \varepsilon_{TM}\frac{\omega(\omega+i\gamma)-1}{\omega(\omega+i\gamma)-\omega_r^2}, \quad (20)$$

$$\text{where } \varepsilon_{TM} = \frac{(a+b)\varepsilon_a\varepsilon_b}{a\varepsilon_b+b\varepsilon_a}, \quad (21)$$

$$\text{and } \omega_r^2 = \frac{b\varepsilon_a}{a\varepsilon_b+b\varepsilon_a}. \quad (22)$$

The associated modes are symmetric. It is important to note that an anti-symmetric mode exists with the following dispersion relation law:

$$\omega(q) = \omega_t , \quad (23)$$

with

$$\omega_t^2 = \frac{a\varepsilon_a}{a\varepsilon_a+b\varepsilon_b}. \quad (24)$$

The frequency of this anti-symmetric mode is thus independent on q and this mode is not coupled to normal incident light.

At this stage, it is possible to compare the previous expressions with those obtained for the ionic crystal model. As in the case of the SPP at one interface ε_{TM}, ω_p, ω_r are respectively the high frequency dielectric constant, the plasma and oscillator frequencies. It is also possible to define by the way of eq. (11) the static dielectric constant

$$\varepsilon_0 = \frac{a+b}{b}\varepsilon_b. \quad (25)$$

As expected, ε_∞ is smaller than ε_0 but contrarily to the SPP at an interface, ε_0 depends on the proportion of the dielectric material in the metamaterial. This is coherent with the fact that ε_0 is due to the contribution of the dielectric material.

In TE field, ε_{eff} follows a Drude model with characteristic dielectric constant, ε_{TE}, and frequency, ω_t. ε_{TE} and ω_t correspond respectively to the average dielectric constant and to the frequency associated to the collective oscillation of the free carrier, that is the plasma frequency or the pseudo volume-plasmon for this metamaterial. Note that ω_t naturally appears in the analytic model.

$$\varepsilon_{eff} = \varepsilon_{TE}\left(1 - \frac{\omega_t^2}{\omega(\omega+i\gamma)}\right), \quad (26)$$

$$\text{with } \varepsilon_{TE} = \frac{(a\varepsilon_a+b\varepsilon_b)}{a+b}. \quad (27)$$

Of course, these results are valid when a and b are smaller than $k_p^{-1}/2$ (see ref. 39 for more details). Indeed for larger thickness, guided modes appear invalidating our main approximation: the long wavelength limit. ω_t can be also view as the cut off frequency of the waveguide.

4. The pseudo volume-plasmon

The main approximation of the analytic model is to consider that we can linearize the tangent function present in the solutions obtained by resolving the Maxwell equations in TM field, respectively for the symmetric (28) and anti-symmetric (29) modes:

$$\varepsilon_b k_a \tan(a\,k_a/2) + \varepsilon_a k_b \left(1 - \frac{1}{\omega(\omega+i\gamma)}\right)\tan(b\,k_b/2) = 0, \quad (28)$$

$$\varepsilon_a k_b \left(1 - \frac{1}{\omega(\omega+i\gamma)}\right)\tan(a\,k_a/2) + \varepsilon_b k_a \tan(b\,k_b/2) = 0. \quad (29)$$

Figure 4 shows the dispersion relation of the optical modes propagating into the metamaterial using the analytic model (open circles) or numerical model (lines or dashed-line eq. 28 and 29). The black and red lines or symbols correspond respectively to the symmetric and the anti-symmetric modes in TM field. The dashed blue line corresponds to the fundamental mode in TE field. As we can see, the analytic model and the numerical one are in very good agreement for $\mathbf{q} < 3.5\ k_p^{-1}$. This upper limit of $\mathbf{q}$ depends directly on the dielectric constant of the constitutive materials of the metamaterial.

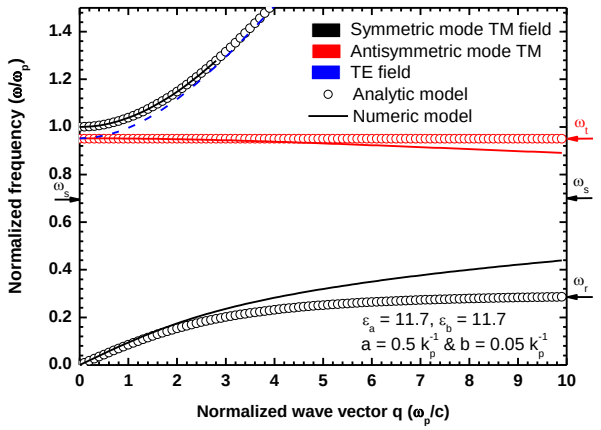

Figure 4: Dispersion relation of SPP into an array of doped and un-doped semiconductors. The dielectric constants are equal to 11.7 and the ratio a/b = 10. The open circle curves correspond to the analytic model. Lines and dashed lines correspond to the numeric model. The dark, red and blue colors correspond respectively to symmetric, anti-symmetric modes in TM filed and the fundamental mode in TE field. The SPP frequency for a single interface is noted ω_s, and ω_t and ω_r are respectively frequencies of the pseudo volume-plasmon and SPP of the analytic model.

We can see that ω_t corresponds exactly to the cut-off frequency for an incident electromagnetic wave in TE field polarization. But in contrast to a waveguide with perfect electric conductor, the cut-off frequency does not depend only on the dielectric constant and on the size of the waveguide, but also on the dielectric constant and on the size of the doped semiconductor (the metal here). This new dependence is mainly due to the fact that the electromagnetic wave penetrates in the metallic part. Indeed, the proximity of the plasma frequency implies a weak permittivity.

By analogy with the case of a metal, ω_t can be interpreted as the plasma or volume plasmon frequency for the metamaterial under investigation. Thus, we define this frequency as the pseudo volume-plasmon frequency, where we use pseudo to differentiate from the rigorous definition of the volume plasmon. This approach allows understanding how modifying the size of both materials modifies ω_t. Decreasing the metal thickness decreases the number of charges and thus ω_t, and vice-versa. At frequencies lower than ω_t, the electromagnetic waves in TE field cannot propagate because the dielectric function is negative. The metal is a perfect mirror. At frequency higher than ω_t, the metal becomes transparent. The electromagnetic waves propagate.

Figure 5 shows a scheme of the pseudo volume-plasmon into the metamaterial. The electric field lines are represented by the black arrows and the charge density is represented by the plus or minus charges for ions and electrons, respectively. This is a longitudinal electric wave with a wavelength λ_t.

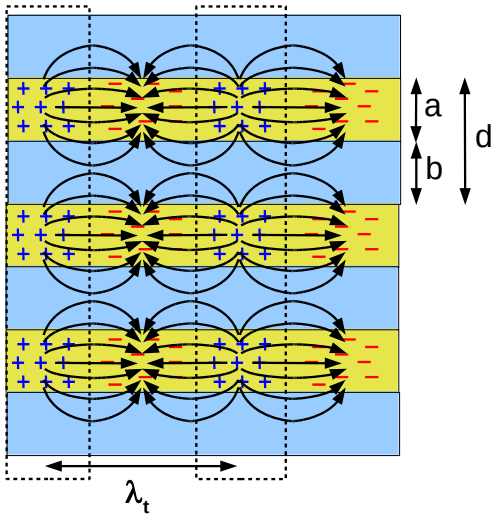

Figure 5: Scheme of the collective oscillation of charges (positive in blue, negative in red) into the metamaterial associated to the pseudo volume-plasmon frequency ω_t and wavelength λ_t. This is a longitudinal wave which is purely electric. The electric field is represented by the black arrows. a, b and d are respectively the thickness of the doped, un-doped semiconductor and the period.

5. Properties of the pseudo volume-plasmon

We will analyse here the behaviour of the pseudo volume-plasmon, particularly near ω_t for $\mathbf{q} = 0$.

Figure 4 shows that at $\mathbf{q} = 0$ there is no degeneracy of the high frequency branches in TE and TM fields ($\omega > \omega_t$). This is not the expected behaviour of a metal.

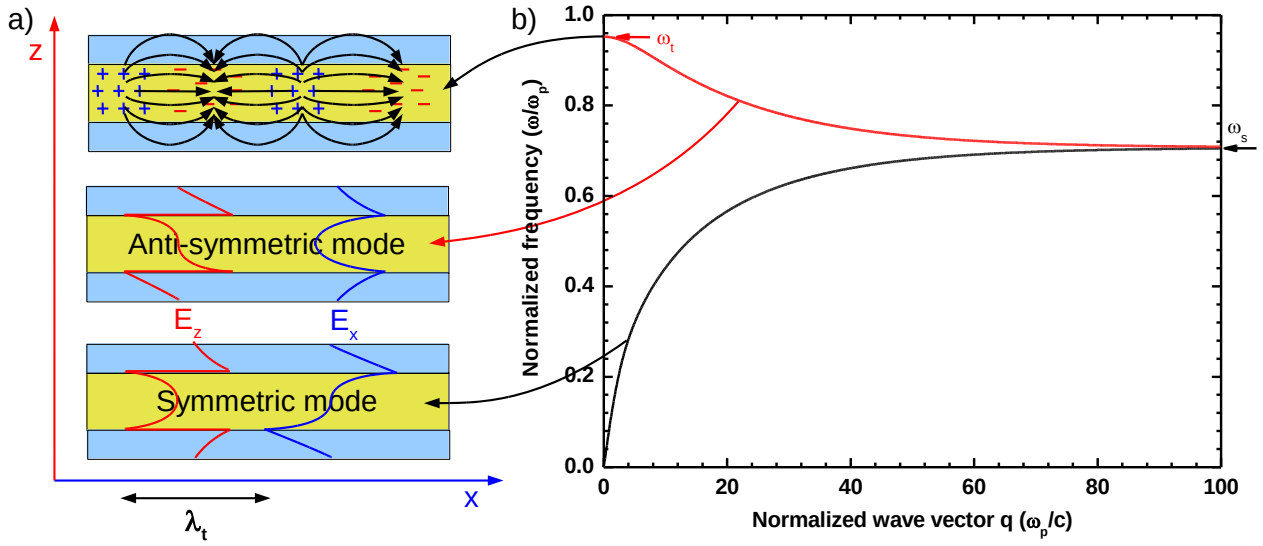

Figure 6: a), b) and c) are respectively schemes of the pseudo volume-plasmon, the anti-symmetric and symmetric modes. The z (red) and x (blue) components of the electric field are depicted. d) Dispersion relations of SPP for the structure shown in fig. 4 obtained with eq. (28)-(29). The dark and red curves correspond respectively to symmetric and anti-symmetric modes in TM filed. The SPP frequency is noted ω_s, and ω_t is the frequency of the pseudo volume-plasmon.

Indeed, if the metamaterial were equivalent to a metal for both polarisations then the lowest frequency of the high frequency mode of the TM field should be resonant with ω_t, the pseudo volume-plasmon frequency.

In contrast to this intuition, the lower frequency of the TM branch is ω_p whereas the cut off frequency of the TE branch is ω_t. In fact, in TE polarization the electromagnetic wave is sensitive to the total carrier concentration into the metamaterial. Thus, the cut-off frequency follows the behaviour of ω_t which depends mainly of the geometry of the metamaterial. In revenge, in TM polarization the low frequency limit of the second symmetric mode depends exclusively on what happens at the metal/dielectric interface. The associated frequency, thus, depends exclusively on the plasma frequency, ω_p, of the metallic part of the metamaterial.

In contrast, fig. 4 reveals unambiguously that the anti-symmetric mode in TM field and the TE mode are degenerated at $\mathbf{q} = 0$. This degeneracy does not depend on the structure except when a and b > 0.5 k_p^{-1} which correspond to the limit of validity of the analytic model [39]. This puzzling behaviour can be explained as follows. Let us first remind the results of the Fig. 2 where we modelled the SPP by an ionic crystal approach. We obtained two solutions for the TM polarisation, one corresponding to the propagative wave with a real wave-vector **q** and the second corresponding to the non-propagative wave with a purely imaginary wave-vector **q**. This second solution mode frequency decreases continuously with **q** from the plasma frequency ω_p to the surface plasmon frequency ω_s. There is a photonic band gap in this frequencies range. In TE polarisation, there is no propagation for $\omega < \omega_p$ whereas propagative waves following the dispersion relation law is possible for $\omega_p < \omega$. It is important to notice that the upper value of the imaginary branch in TM field is equal to the lower value of the real branch in TE field, that is ω_p, for $\mathbf{q} = \mathbf{0}$. Now, there is an analogy between the ionic crystal and the doped/undoped semiconductor periodic array. In the case of the periodic structures (Fig. 6-d), the plasma frequency ω_p is replaced by the pseudo volume-plasmon, ω_t, depicted in the Fig. 6-a. In TE field, the propagative waves are allowed for $\omega < \omega_t$. In TM field, we obtain two propagative modes for $\omega < \omega_t$, one symmetric and the other one anti-symmetric. But in contrast to the two dimensional case with SPP, the imaginary branch is real which means that both modes propagate. If we compare the dispersion relations of the metal/dielectric interface (Fig. 2) and of the metamaterial at high **q** (Fig. 6-b) we obtain the same behaviour. The upper and lower limit frequencies for the imaginary mode in TM field and the anti-symmetric mode in TM field are identical, ω_p or ω_t and ω_s, respectively. So the anti-symmetric mode of the metamaterial corresponds to the imaginary mode in TM field.

The question is whether this situation is physically sound. In fact, it is the periodicity of the structure that transforms the imaginary solution into a real one. Indeed, an anti-symmetric mode has no meaning at a metal/dielectric interface. Only a symmetric mode can exist (Fig. 6-c). In revenge, anti-symmetric mode is possible in periodic structures because of the possibility to pin the electric field at the interfaces and to extinguish the electric field into the dielectric or metallic part of the metamaterial (Fig. 6-b). When the frequency of this anti-symmetric mode reaches ω_t

its longitudinal component become dominant leading to a mode which is not coupled to incident light. This is the definition of the pseudo volume-plasmon.

At this stage, it is interesting to evaluate how modifying the properties of the metamaterial (a, b, n_a and n_b) impacts ω_t the pseudo volume-plasmon. The general expression of the volume plasmon when positive charges are immersed in a material with a dielectric constant ε is:

$$\omega_p = \sqrt{\frac{ne^2}{m\varepsilon\varepsilon_0}}, \qquad (30)$$

where n and m are respectively the charge density and the electron effective mass. To modify ω_p, one can play with n, m or ε. As an example, consider dividing the charge density by a factor 2. Eq. (30) shows that ω_p will be divided by $\sqrt{2}$. Now, consider a periodic structure with $\varepsilon_a = \varepsilon_b$, and a = b. Eq. (24) leads to $\omega_t = \frac{1}{\sqrt{2}}$ which means that ω_t is also divided by $\sqrt{2}$. This is a confirmation of the same behaviour for both equations.

These results show that one can easily control ω_t just by modifying the geometrical properties of the metamaterial or by changing the individual materials constituting the periodic array, *i.e.* changing the dielectric constants. This is a very important asset of our system. In the case of metals, it is very difficult to play directly with these parameters to reach wavelength in the IR range. One of the main solution is to consider a metamaterial composed of metallic nano-particles (NP) embedded in host material [40]. Indeed, if the electromagnetic wave averages the metamaterial, changing the size and the density of NP allows playing with the electron density. But it is very difficult to control exactly what occurs in terms of charge density, dielectric constant and homogeneity of the material. In the case of doped semiconductors in contrast, one can select the right semiconductors and adjust at will their doping level to obtain the target m and ε. Eq. (24) shows that in the general case when a, b, ε_a and ε_b can be adjusted, achieving a target volume plasmon frequency is trivial whereas it is not so simple with metals (Eq. (30)). Our simplified model can be used to easily design and fabricate a metamaterial with the expected optical properties. Of course, doped semiconductors cannot be used in the visible range. However, they can be the best choice for IR applications.

6. Summary and conclusion

After having presented the analogy between surface plasmon polaritons and the ionic-cristal model in the case of a single interface and a periodic array of metal/dielectric system, we have shown that an analytic model allows defining a pseudo volume-plasmon frequency, ω_t, associated to the periodic array. By adjusting the physical properties of the structure (a, b, n_a, n_b) it is thus possible to define the characteristic frequencies ω_r, ω_t and ω_s, and to control their optical properties. We have explained the behaviour of ω_t as a function of the physical parameters. We have also explained why ω_t corresponds to the cut off frequency in TE Field and to the high frequency limit of the anti-symmetric mode in TM field.

References

[1] S. A. Maier, "Plasmonics: Fundamentals and Applications", Springer Science+Buisness Media LLC (2007).

[2] A. V. Zayats, I. I. Smolyaninov, A. A. Maradudin, "Nano-optics of surface plasmon polaritons" Physics Reports **408**, 131–314 (2005)

[3] D. K. Gramotnev and S. I. Bozhevolnyi, "Plasmonics beyond the diffraction limit" Nature Photonics **4**, 83 - 91 (2010).

[4] S. C. Kitson, W. L. Barnes, and J. R. Sambles, "Full Photonic Band Gap for Surface Modes in the Visible" Physical Review Letters **77**, 2670–2673 (1996).

[5] S. I. Bozhevolnyi, J. Erland, K. Leosson, P. M. W. Skovgaard, and J. M. Hvam, "Waveguiding in Surface Plasmon Polariton Band Gap Structures" Physical Review Letters **86**, 3008–3011 (2001).

[6] T. W. Ebbesen, H. J. Lezec, H. F. Ghaemi, T. Thio, and P.A. Wolff, "Extraordinary optical transmission through sub-wavelength hole arrays" Nature **391**, 667, (1998).

[7] V. V. Temnov, G. Armelles, U. Woggon, D. Guzatov, A. Cebollada, A. Garcia-Martin, J.-M. Garcia-Martin, T. Thomay, A. Leitenstorfer and R. Bratschitsch, "Active magneto-plasmonics in hybrid metal–ferromagnet structures" Nature Photonics **4**, 107 - 111 (2010).

[8] Y. Pu, R. Grange, C.-L. Hsieh, and D. Psaltis, "Nonlinear Optical Properties of Core-Shell Nanocavities for Enhanced Second-Harmonic Generation" Physical Review Letters **104**, 207402 (2010).

[9] S. Kim, J. Jin, Y.-J. Kim, I.-Y. Park, Y. Kim and S.-W. Kim "High-harmonic generation by resonant plasmon field enhancement" Nature 453, 757-760 (2008).

[10] R. D. Kekatpure, E. S. Barnard, W. Cai, and M. L. Brongersma, "Phase-Coupled Plasmon-Induced Transparency" Physical Review Letters **104**, 243902 (2010).

[11] T. Utikal, M. I. Stockman, A. P. Heberle, M. Lippitz, and H. Giessen, "All-Optical Control of the Ultrafast Dynamics of a Hybrid Plasmonic System" Physical Review Letters **104**, 113903 (2010).

[12] R.H. Ritchie, "Plasma losses by fast electrons in thin films" Physical Review **106**, 874 (1957).

[13] C.J. Powell, and J.B. Swan, "Effect of oxidation on the characteristic loss spectra of aluminium and magnesium" Physical Review **118**, 640 (1960).

[14] E.A. Stern, and R.A. Ferrel, "Surface plasma oscillations of a degenerate electron gas" Physical Review **120**, 130 (1960).

[15] Y.B. Li, R. A. Stradling, T. Knight, J. R. Birch, R. H. Thomas, C. C. Philips and I. T. Ferguson, "Infrared reflection and transmission of undoped and Si-doped InAs grown on GaAs by molecular beam epitaxy" Semiconductor Science Technology **8**, 101-111 (1993).

[16] J. B. Pendry, A. J. Holden and W. J. Stewart and I. Youngs, "Extremely Low Frequency Plasmons in Metallic Mesostructures" Physical Review Letters 76, 4773 (1996).

[17] P. A. Belov, C. R. Simovski, and S. A. Tretyakov, "Two-dimensional electromagnetic crystals formed by reactively loaded wires", Physcial Review E **66**, 036610 (2002).
[18] R. Marques, J. Martel, F. Mesa, and F. Medina, "Left-Handed-Media Simulation and Transmission of EM Waves in Subwavelength Split-Ring-Resonator-Loaded Metallic Waveguides" Physical Review Letters **89**, 183901 (2002).
[19] U. Shröter and D. Heitmann, "Surface-plasmon-enhanced transmission through metallic gratings" Physical Review B **58**, 15419 (1998).
[20] J.A. Porto, F. J. Garcia-Vidal, and J. B. Pendry, "Transmission Resonnances on Metallic Gratings with Very Narrow Slits" Physical Review Letters **83**, 2845 (1999).
[21] F. J. Garcia-Vidal, L. Martin-Moreno, T. W. Ebbesen, and L. Kuipers, "Light passing through subwavelength apertures" Reviews of Modern Physics **82**, 729 (2010).
[22] R. E. Camley and D. L. Mills, "Collective excitations of semi-infinite superlattice structures : Surface plasmons, bulk plasmons, and the electron-energy-loss spectrum" Physical Review B **29**, 1695 (1984).
[23] R. Szenics, R.F. Wallis, G.F. Giuliani, and J.J. Quinn, "Theory of surface plasmon polaritons in truncated superlattices" Surface Sciences **166**, 45 (1986).
[24] R.F. Wallis, R. Szenics, J.J. Quinn, and G.F. Giuliani, "Theory of surface magnetoplasmon polaritons in truncated superlattices" Physical Review B **36**, 1218 (1987).
[25] R.F. Wallis and J.J. Quinn, "Surface magnetoplsamon polaritons in truncated semiconductor superlattices" Physical Review B **38**, 4205 (1988).
[26] J. Léon and T. Taliercio, "Large tunable photonic band gaps in nanostructured doped semiconductors" Physical Review B **82**, 195301 (2010).
[27] E. N. Economou, "Surface Plasmons in Thin Films" Physical Review **182**, 539–554 (1969).
[28] J. J. Burke, G. I. Stegeman, and T. Tamir, "Surface-polariton-like waves guided by thin, lossy metal films" Physical Review B **33**, 5186 (1986).
[29] B. Prade, J. Y. Vinet, and A. Mysyowicz, "Guided optical waves in planar heterostructures with negative dielectric constant" Physical Review B **44**, 13556 (1991).
[30] A. J. Hoffman, L. Alekseyev, S. S. Howard, K. J. Franz, D. Wasserman, V. A. Podolskiy, E. E. Narimanov, D. L. Sivco, and C. Gmachl, "Negative refraction in semiconductor metamaterials" Nature Materials **6**, 946 (2007).
[31] A. J. Hoffman, A. Sridhar, P. X. Braun, L. Alekseyev, S. S. Howard, K. J. Franz, L. cheng, F. S. Choa, D. L. Sivco, V. A. Podolskiy, E. E. Narimanov, and C. Gmachl, "Midinfrared semiconductor optical metamaterials" Journal of Applied Physics **105**, 122411 (2009).
[32] E. Verhagen, R. de Waele, L. Kuipers, and A. Polman, "Three-dimensional negative index of refraction at optical frequencies by coupling plasmonic waveguides" Physical Review Letters **105**, 223901 (2010).
[33] H. J. Lezec, J. A. Dionne, and H. A. Atwater, "Negative refraction at visible frequencies" Science **316**, 430 (2007).
[34] J. A. Dionne, E. Verhagen, A. Polman, and H. A. Atwater, "Are negative index materials achievable with surface plasmon waveguides? A case study of three plasmonic geometries" Optics express **16**, 19001 (2008).
[35] J. T. Shen, P. B. Catrysse, and S. Fan "Mechanism for Designing Metallic Metamaterials with a High Index of Refraction" Physical Review Letters **94**, 197401 (2005).
[36] J. Gomez Rivas, M. Kuttge, P. Haring Bolivar, H. Kurz, and J. A. Sanchez-Gil "Propagation of surface plasmon polaritons on semiconductor gratings" Physical Review Letters **93**, 256804 (2004).
[37] J. Gomez Rivas, M. Kuttge, H. Kurz, P. Haring Bolivar, and J. A. Sanchez-Gil, "Low-frequency active surface plasmon optics on semiconductors" Applied Physics Letters **88**, 082106 (2006).
[38] N. W. Ashcroft and N. D. Mermin, "Solid state physics", Saunders College Publishing, Orlando, FL, first edition (1976).
[39] T. Taliercio, V. N'Tsame Guilengui, J. Léon and E. Tournié "Analytical model to describe the optical properties of arrays of doped and un-doped semiconductors" in preparation.
[40] C.-P. Huang, X.-G. Yin, Q.-J. Wang, H. Huang, and Y.-Y. Zhu, "Long-Wavelength Optical Properties of a Plasmonic Crystal" Physical Review Letters **104**, 016402 (2010).